AIP | Applied Physics Letters

# A two-step plasma processing for gold nanoparticles supported on silicon near-infrared plasmonics

Giovanni Bruno, Giuseppe V. Bianco, Maria M. Giangregorio, Alberto Sacchetti, Pio Capezzuto et al.

Citation: Appl. Phys. Lett. **96**, 043104 (2010); doi: 10.1063/1.3291670
View online: http://dx.doi.org/10.1063/1.3291670
View Table of Contents: http://apl.aip.org/resource/1/APPLAB/v96/i4
Published by the American Institute of Physics.

# A two-step plasma processing for gold nanoparticles supported on silicon near-infrared plasmonics

Giovanni Bruno,[a] Giuseppe V. Bianco, Maria M. Giangregorio, Alberto Sacchetti, Pio Capezzuto, and Maria Losurdo
*Department of Chemistry, Institute of Inorganic Methodologies and of Plasmas, IMIP-CNR, University of Bari, via Orabona 4, 70126 Bari, Italy*

(Received 24 November 2009; accepted 11 December 2009; published online 25 January 2010)

A *two-step* sputtering methodology for fabricating gold nanoparticles supported on silicon with tuneable surface plasmon resonance down to the near-infrared spectral range has been developed. This methodology uses modification of the wettability of Si surfaces by an intermediate $O_2$ plasma treatment to decouple diameter and height of nanoparticles as tuneable parameters to tailor the plasmon resonance. © *2010 American Institute of Physics*. [doi:10.1063/1.3291670]

Plasmonics is a rapidly developing field in nanoscience.[1] The interest in the size-dependent properties of plasmonic noble metal particles, i.e., gold and silver, is driven by the large number of innovative applications including biosensors,[2,3] photonic,[4,5] optoelectronic[6] and photovoltaic devices,[7] and substrates for surface-enhanced Raman spectroscopy (SERS),[8] and substrates for the catalyzed vapor-liquid-solid (VLS) growth of ordered unidimensional nanostructures.[9]

These applications require the metal nanoparticles (NPs) to exhibit the surface plasmon resonance (SPR) and to be supported on a substrate, and their further development relies on the production of NPs with controlled SPR properties assembled on technological important substrates.

Recently, there has also been increasing interest for plasmonic metal nanostructures with SPR in the mid-infrared (mid-IR) range.[10] Au nanospheres over a broad range of size have a resonance in the range 520–580 nm (2.1–2.4 eV),[11] while nanostructures with high aspect ratio such as nanorods[12] are considered for plasmon tunability in the near infrared. Gold nanorods depending on their aspect ratio can yield a longitudinal SPR mode down to 1.2 eV.[13]

Several bottom-up and top-down synthesis methodologies are used to create two dimension NP systems exhibiting specific SPR properties, including self-assembling by Au NPs colloidal solutions,[14] electrochemical methods,[15] physical vapor deposition (PVD) methods, e.g., thermal evaporation, sputtering,[16] laser ablation,[17] also using patterned substrates,[18] and the preparation of NPs arrays by lithographic techniques.[19] However, the patterns accessible by lithography have characteristic length scales of a few 100 nm, exceeding the dimensions ideal for SERS by one order of magnitude, and colloidal metal NPs are difficult to assemble into dense and extended two-dimensional layers if they have diameters in the sub-100 nm range or if they have nonspherical shapes.

Although PVD methodologies application is limited by a low NPs size and spacing control, they present advantages of being dry processes compatible with most of device technologies and substrates of technological interest. All the previous studies have demonstrated that the SPR excited in a particle is strongly dependent on the surrounding environment such as neighboring particles or the substrate. Therefore, for substrate-supported NPs, surface treatments and modifications can be used as an additional degree of freedom to tailor SPR wavelength. In the case of Au NPs supported on a silicon substrate, interface characteristics such as residual $SiO_2$ and/or gold silicide formation,[20] affect system structure and SPR properties.

This work demonstrates the viability of a sputtering methodology for obtaining gold NPs supported on c-Si (111) with a tunable SPR ranging from 551 to 800 nm. This sputtering methodology consists of a *two-step* Au deposition including a Si-oxidation intermediate step according to the process sequence schematized in Fig. 1. Specifically, in the first step, Au NPs seeds are created on the silicon surface by sputtering and annealing an Au amount of a few monolayers

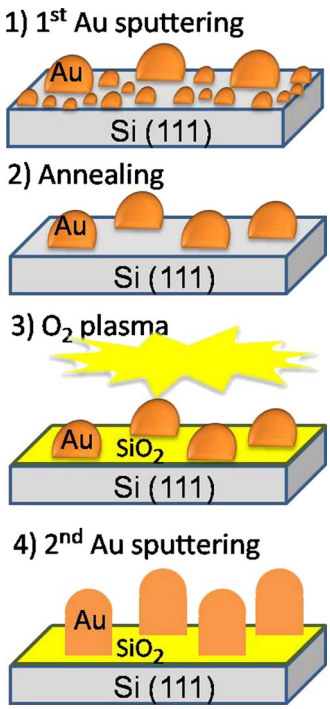


FIG. 1. (Color online) Schematic representation of the two-step sputtering process of Au NPs. (1) Au sputtering to nucleate metal seeds; (2) annealing; (3) $O_2$ plasma; and (4) second sputtering step to tailor NPs size.

[a]Author to whom correspondence should be addressed. Electronic mail: giovanni.bruno@ba.imip.cnr.it. Tel.: +39-0805442094-2007. FAX: +39-0805443562.

 

(MLs) (<20 MLs). Once those Au NPs seeds are created, an $O_2$ plasma is applied to oxidize the silicon surface uncovered by the Au seeds. Finally, a second Au sputtering step is performed to enlarge the preformed Au seeds. The impact of this two-step methodology and of the $O_2$ plasma treatment on the NPs growth dynamic and resulting SPR is presented, and a comparison of Au NPs SPR for samples produced with and without the described two-step methodology are discussed. It is demonstrated that this *two-step* methodology provides a reliable and reproducible way to decouple the tunability of diameter and height of NPs, and, hence, to tailor the SPR down to the near-infrared range.

Au NPs were deposited by rf (13.56 MHz) sputtering an Au target using an Ar plasma under a dc self-bias potential of −500 V. The Au sputtered MLs were controlled by the sputtering time. c-Si(111) was used as substrate. After removal of the native oxide by etching in a HF (1%) solution for 2 min, the substrate were immediately loaded into the ultrahigh vacuum (UHV) reactor and further degassed at 350 °C.

Two sets of samples were produced: some samples were obtained by a *single-step* sputtering of Au at 350 °C for a time ranging between 500 and 1500 s; *two-step* sputtering samples were obtained by (1) a first Au sputtering step at 150 °C for 50–200 s followed by (2) Au nuclei annealing at 150 °C for 1 h and (3) a rf (13.56 MHz) $O_2$ plasma (rf power=50 W; pressure=0.3 Torr) for 1 h and, subsequently, (4) a second sputtering step at 350 °C for 300–1200 s, as shown in the scheme of Fig. 1.

Optical characterization was performed exploiting spectroscopic ellipsometry (SE).[21] SE measurements of the pseudoextinction coefficient, ⟨k⟩, of the Au NPs ensemble on Si(111) were performed in the range 190–1700 nm (0.75–6.5 eV) with a phase modulated spectroscopic ellipsometer (UVISEL-Jobin Yvon) at an incidence angle of 70°.

Non-contact intermittent mode atomic force microscopy was used for sizing of NPs using an AutoProbe CP Thermomicroscope. A high aspect ratio probe-super sharp tip with a radius of curvature of 2 nm (ESP Series Probes-VEECO) was used to reduce the convolution effect of the tip on the lateral size of NPs.

Figure 2 shows the comparison of the SE experimental spectra of the pseudoextinction coefficients of the ensemble of Au NPs produced by the single-step sputtering (open symbols) and by the *two-step* sputtering (fill symbols) with a total sputtering time of 1000 and 1500 s, corresponding to 100 and 150 MLs of Au, respectively. In the spectral region above 3 eV, SE spectra are characterized by the $E_1$ and $E_2$ critical points (CPs) of c-Si,[22] whose amplitude decreases with the increase in the Au MLs. Below 3 eV, spectra are characterized by the SPR peak whose wavelength and amplitude changes according to the Au MLs, the different experimental processing and, hence, the different NPs geometry. Specifically, for Au NPs produced by the *two-step* methodology, a strong redshift of the SPR peak and an increase in the SPR amplitude is observed.

Figure 2 also shows the comparison of AFM images of samples produced by the *single-step* and two-step sputtering for a total amount of Au 100 MLs. Indeed, the *two-step* methodology results in a smaller diameter but higher NPs whose height mainly increases with time, whereas the one-step methodology yields mainly flat larger NPs whose diameter mainly increases with sputtering time.

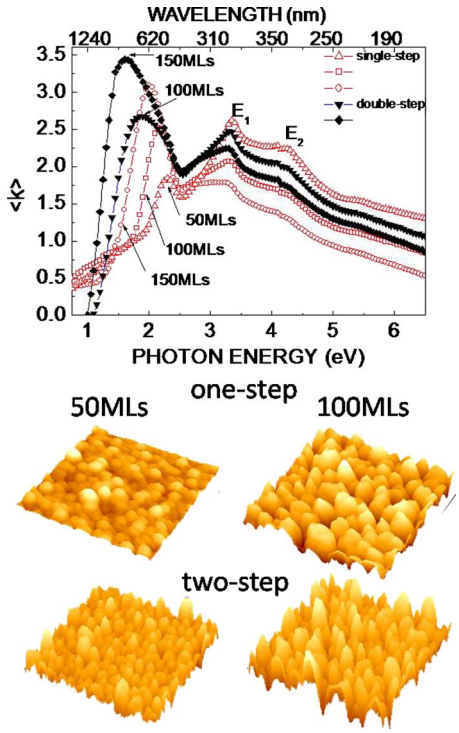


FIG. 2. (Color online) SE experimental spectra of the pseudoextinction coefficients of NPs films produced by Au sputtering of 50–150 MLs of Au on c-Si (111) exploiting the *single-step* sputtering (open symbols) and the *two-step* sputtering methodology (full symbols). The three-dimensional (3D) $500\times500$ nm$^2$ AFM images of Au NPs corresponding to 50 and 100 MLs of Au deposited by the *single-step* and the *two-step* sputtering are also shown. For all AFM images vertical scale is the same of 40.97 nm.

The correlation between the different geometry of the NPs and resulting SPR wavelength is summarized in Fig. 3. Here, the SPR position is reported as a function of the diameter and of the height of NPs obtained by the one-step and the two-step sputtering processes. The common diameter region corresponds to the initial nuclei-seeds formation (the first 5–20 MLs) of both processes (the dashed box in Fig. 3). In the one-step conventional sputtering, the diameter tends to increase toward lateral coalescence of island. Therefore, by the conventional sputtering is not possible to increase the sputtering time to redshift continuously the Au SPR. When gold is deposited by the one-step sputtering, only a slight redshift of 100 nm is observed by increasing the diameter of NPs by one order of magnitude. Conversely, in the two-step sputtering soon after the $O_2$ plasma is run and the second sputtering step applied, the $SiO_2$ acts as a kind of surface mask for further Au nucleation alloying height growth of the already formed nuclei. Therefore, the NPs diameter stays almost constant and the height increases yielding to elongated asymmetric NPs (see also Fig. 3) with a redshifting SPR.

Thus, the two-step sputtering methodology can be used to control independently height and diameter of Si-supported Au NPs.

Interestingly, these results are in agreement with the use of an oxide buffer layer to confine the metal growth on a patterned surface and localize the metal island reported by Atwater's group.[9]

In order to elucidate the different growth mode of NPs during the two-step sputtering, we have been considering the modification of the surface/interface chemistry. The interface chemistry between the Si substrate and the Au NPs has been

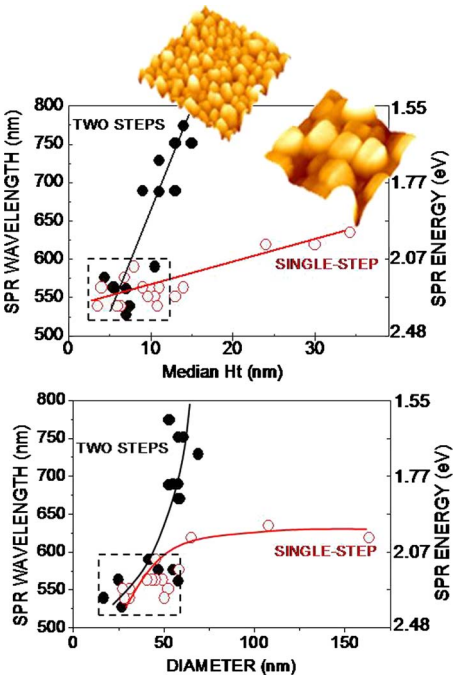


FIG. 3. (Color online) Dependence of the SPR wavelength and energy on the Median height and on the diameter, as determined from AFM analysis of Au NPs deposited by the *single-step* (empty symbols) and the *two-step* (full symbols) sputtering methodologies. The dashed square indicates the regime of nucleation of Au seeds (i.e., the first <20 ML Au similarly deposited for the two methodologies). The $500\times500$ nm$^2$ AFM images for typical Au NPs samples deposited by the single-step and two-step sputtering are also shown. In the 3D AFM images, the vertical scale is 45.17 nm for both.

characterized by x-ray photoelectron spectroscopy and corroborated by SE spectra modeling. In particular, a $6.1\pm0.3$ nm thick interface composed by an Au-Si alloy has been found for the samples produced by the *single-step* sputtering, due to gold diffusion into the substrate, which, according to a previous study could be assigned to a crystalline precipitates of metastable $Au_4Si$ phase.[23]

Conversely, samples produced with the *two-step* methodology and treated with the $O_2$ plasma, a $8.6\pm0.3$ nm thick NPs/c-Si interface composed mostly by $SiO_2$ (81%) and Au-Si alloy (19%) has been found.

Therefore, it is inferred that the different morphology of Au NPs produced by the *two-step* methodology mainly stems from the presence of this oxide layer that modify the growth mode of NPs. Specifically, since the formation energy of nuclei decreases with decreasing surface tension, and being the surface tension for Si (0.78 J/m$^2$) lower than that of $SiO_2$ (1.5 J/m$^2$),[24] the higher energy of formation of particles nuclei on $SiO_2$ than on c-Si inhibits further Au NPs nucleation during the second sputtering step, favoring, on the other hand, gold adatom diffusion toward *seed*s preformed in the first sputtering step. This is also in agreement with previous finding reporting that Au does not wet the $SiO_2$ surface and that contact angle of 140° have been experimentally reported for Au on $SiO_2$.[25] Furthermore, while the Au condensation coefficient on Si(111) remains unity up to 700 °C,[26] a *condensation coefficient* below unity[27] for Au on $SiO_2$ contributes to maximizing the condensation of metal-on-metal, and, hence, to the increase mainly of height of Au NPs during the second-step of sputtering.

In conclusion, a *two-step* sputtering methodology that includes an intermediate $O_2$ plasma treatment of the Si surface, is a valuable dry synthesis procedure to control the nucleation and position of the Au NPs on Si substrates. This methodology provides a full-device technology compatible way to deposit even on large scale plasmonic Au/Si systems with a SPR tunable down to the near-infrared. This methodology exploits the difference in Au sticking coefficient on Si and $SiO_2$ surfaces. By using this kind of $SiO_2$ masking effect, the vertical and lateral growth of Au NPs by sputtering can be decoupled. Therefore, strongly asymmetric particles with a high shape factor can be deposited directly onto Si surfaces and controlling their height to tailor the SPR.

This work has been supported by the European Community's Seventh Framework Programme under the project NanoCharM (Grant No. NMP3-CA-2007-218570).

[1] J. Heber, Nature (London) **461**, 720 (2009).
[2] C. Sönnichsen and A. P. Alivisatos, Nano Lett. **5**, 301 (2005).
[3] T. J. Wang and W. S. Lin, Appl. Phys. Lett. **89**, 173903 (2006).
[4] E. Verhagen, M. Spasenovic, A. Polman, and L. Kuipers, Phys. Rev. Lett. **102**, 203904 (2009).
[5] R. F. Oulton, F. Oulton, V. J. Sorger, T. Zentgraf, R.-M. Ma, C. Gladden, L. Dai, G. Bartal, and X. Zhang, Nature (London) **461**, 629 (2009).
[6] J. A. Dionne, K. Diest, L. A. Sweatlock, and H. A. Atwater, Nano Lett. **9**, 897 (2009).
[7] M. Losurdo, M. M. Giangregorio, G. V. Bianco, A. Sacchetti, P. Capezzuto, and G. Bruno, Sol. Energy Mater. Sol. Cells **93**, 1749 (2009).
[8] D. L. Jeanmaire and R. P. Van Duyne, J. Electroanal. Chem. **84**, 1 (1977).
[9] B. M. Kayes, M. A. Filler, M. C. Putnam, M. D. Kelzenberg, N. S. Lewis, and H. A. Atwater, Appl. Phys. Lett. **91**, 103110 (2007).
[10] A. C. Jones, R. L. Olmon, S. E. Skrabalak, B. J. Wiley, Y. N. Xia, and M. B. Raschke, Nano Lett. **9**, 2553 (2009).
[11] B. Balamurugan and T. Maruyama, Appl. Phys. Lett. **87**, 143105 (2005).
[12] S. Link and M. A. El-Sayed, J. Phys. Chem. B **103**, 8410 (1999).
[13] S. Link, M. B. Mohamed, and M. A. El-Sayed, J. Phys. Chem. B **103**, 3073 (1999).
[14] P. T. Hammond, Adv. Mater. **16**, 1271 (2004).
[15] Y.-Y. Yu, S.-S. Chang, C.-L. Lee, and C. R. C. Wang, J. Phys. Chem. B **101**, 6661 (1997).
[16] X. Zhou, Q. Wei, K. Sun, and L. Wang, Appl. Phys. Lett. **94**, 133107 (2009).
[17] S. H. Ko, Y. Choi, D. J. Hwang, C. P. Grigoropoulos, J. Chung, and D. Poulikakos, Appl. Phys. Lett. **89**, 141126 (2006).
[18] B. Ressel, K. C. Prince, S. Heun, and Y. Homma, J. Appl. Phys. **93**, 3886 (2003).
[19] P. K. Jain, W. Huang, and M. A. El-Sayed, Nano Lett. **7**, 2080 (2007).
[20] C.-L. Kuo and P. Clancy, Surf. Sci. **551**, 39 (2004).
[21] M. Losurdo, M. Bergmair, G. Bruno, D. Cattelan, C. Cobet, A. de Martino, K. Fleischer, Z. Dohcevic-Mitrovic, N. Esser, M. Galliet, R. Gajic, D. Hemzal, K. Hingerl, J. Humlicek, R. Ossikovski, Z. V. Popovic, and O. Saxl, J. Nanopart. Res. **11**, 1521 (2009).
[22] D. E. Aspnes and A. A. Studna, Phys. Rev. B **27**, 985 (1983).
[23] Z. Ma and L. H. Allen, Phys. Rev. B **48**, 15484 (1993).
[24] C. V. Thompson and R. Carel, Mater. Sci. Eng., B **32**, 211 (1995).
[25] C. L. Kuo and P. Clancy, Modell. Simul. Mater. Sci. Eng. **13**, 1309 (2005).
[26] J. Westwater, D. P. Gosain, and S. Udui, Phys. Status Solidi A **165**, 37 (1998).
[27] A. A. Schmidt, H. Eggers, K. Herwig, and R. Anton, Surf. Sci. **349**, 301 (1996).